C. R. Geoscience 350 (2018) 4–12

Contents lists available at ScienceDirect

Comptes Rendus Geoscience

www.sciencedirect.com

Hydrology, Environment

Spatio-temporal monitoring of suspended sediments in the Solimões River (2000–2014)

Raul Espinoza-Villar [a,*], Jean-Michel Martinez [b], Elisa Armijos [c], Jhan-Carlo Espinoza [d], Naziano Filizola [e], Andre Dos Santos [e,f], Bram Willems [a], Pascal Fraizy [b], William Santini [b], Philippe Vauchel [b]

[a] Facultad de Ciencias Fisicas, UNMSM, 15081 Lima, Peru
[b] GET, UMR5563, CNRS/IRD/université Toulouse-3, 31400 Toulouse, France
[c] CLIAMB-Instituto Nacional de Pesquisas da Amazônia–Universidade do Estado do Amazonas, 69.060-001 Manaus, Brazil
[d] Instituto Geofísico del Perú, 15026 Lima, Peru
[e] Laboratório de Potamologia Amazônica, UFAM, 69.067-000 Manaus, Brazil
[f] Serviço Geológico do Brasil (CPRM), 69.067-375 Manaus, Brazil

ARTICLE INFO

Article history:
Received 3 June 2016
Accepted after revision 11 May 2017
Available online 20 June 2017

Handled by François Chabaux

Keywords:
Sediment transport
Remote sensing
Modis
Radiometry

ABSTRACT

The Amazon River sediment discharge has been estimated at between 600 and 1200 Mt/year, of which more than 50% comes from the Solimões River. Because of the area's inaccessibility, few studies have examined the sediment discharge spatial and temporal pattern in the upper Solimões region. In this study, we use MODIS satellite images to retrieve and understand the spatial and temporal behaviour of suspended sediments in the Solimões River from Peru to Brazil. Six virtual suspended sediment gauging stations were created along the Solimões River on a 2050-km-long transect. At each station, field-derived river discharge estimates were available and field-sampling trips were conducted for validation of remote-sensing estimates during different periods of the annual hydrological cycle between 2007 and 2014. At two stations, 10-day surface suspended sediment data were available from the SO-HYBAM monitoring program (881 field SSS samples). MODIS-derived sediment discharge closely matched the field observations, showing a relative RMSE value of 27.3% (0.48 Mtday) overall. Satellite-retrieved annual sediment discharge at the Tamshiyacu (Peru) and Manacapuru (Brazil) stations is estimated at 521 and 825 Mt/year, respectively. While upstream the river presents one main sediment discharge peak during the hydrological cycle, a secondary sediment discharge peak is detected downstream during the declining water levels, which is induced by sediment resuspension from the floodplain, causing a 72% increase on average from June to September.

1. Introduction

Amazon River sediment discharge is controlled by the slope, soil type, climate, geology and morphology of the catchment (Dunne et al., 1998; Mertes et al., 1996) and may now experience significant influence of anthropogenic activities, such as land-use change related to deforestation, industrial activity, gold mining, or dam constructions.

The Amazon River drains an area greater than 6.5×10^6 km^2; the mean discharge at the river mouth in the Atlantic Ocean is 209,000 m^3/s (Molinier et al., 1996). The Amazon River is formed in Peru, at the confluence of

* Corresponding author.
E-mail address: respinozavillar@gmail.com (R. Espinoza-Villar).

http://dx.doi.org/10.1016/j.crte.2017.05.001
1631-0713/

the Ucayali and Marañón rivers, and is renamed the Solimões River at the Peruvian–Brazilian border. It is only 2050 km downstream, at the confluence of the Solimões and Negro rivers, that the river is called the Amazon again. The Amazon River is the world's largest fluvial system in terms of drainage area and runoff. At the gauging station at the city of Óbidos, sediment discharge was estimated at 600–1200 Mt/year (Filizola, 2003; Filizola et al., 2011; Gibbs, 1967; Meade et al., 1979; Guyot et al., 2005; Martinez et al., 2009).

Amazon River sediment discharge is mainly supplied by the Madeira sub-catchment (48%) and Solimões sub-catchment (50%) (Filizola, 1999). Besides its dominance in terms of the liquid, solid and dissolved contribution to the Amazon basin's inputs to the Atlantic Ocean, the dynamic of suspended sediment along the Solimões River 1600-km long stretch is known little, apart from results provided by the HYBAM long-term monitoring program at Tamshiyacu, Tabatinga and Manacapuru stations and some field-sampling trips in the 1980s and 1990s (Dunne et al., 1998, Guyot et al., 1998; Richey et al., 1986).

The Tamshiyacu gauging station (TAM) is located at 85 km downstream from the confluence of the Ucayali and Marañón rivers in Peru (Fig. 1). River discharge at the TAM station represents 16% of the mean water discharge at the mouth of the Amazon River (Espinoza et al., 2009, 2011, 2012; Ronchail et al., 2006) and 400–550 Mt/year of sediments discharge (Armijos et al., 2013; Guyot et al., 2007).

Downstream, at the Manacapuru gauging station (MNA, Fig. 1), the last station before the Negro River confluence, the Solimões River discharge is 103,000 m^3/s, approximately three times the river discharge at TAM station, which denotes a significant contribution in terms of water balance of local tributaries such as the Napo, Japura, Jurua, Javari, and Purus Rivers. At the MNA station, river sediment discharge has been calculated at between 400 and 700 Mt/year (Dunne et al., 1998, Filizola, 1999, 2003; Filizola and Guyot, 2009; Laraque et al., 2005). Therefore, there appears to be little or no increase in sediment discharge along the Solimões River stretch, although many tributaries drain geomorphological areas that are subject to significant erosion processes, such as the northern Andes of Ecuador and Colombia (e.g., Napo, Iça, Japura Rivers) and the Fitzcarrald Arch (mainly Jurua and Purus Rivers). Important questions remain, including the role of the large Solimões River floodplain and the sediment discharge dynamics of the main tributaries. The use of alternative techniques for suspended sediment monitoring is important for filling gaps in our current understanding of the main tributary of the Amazon River.

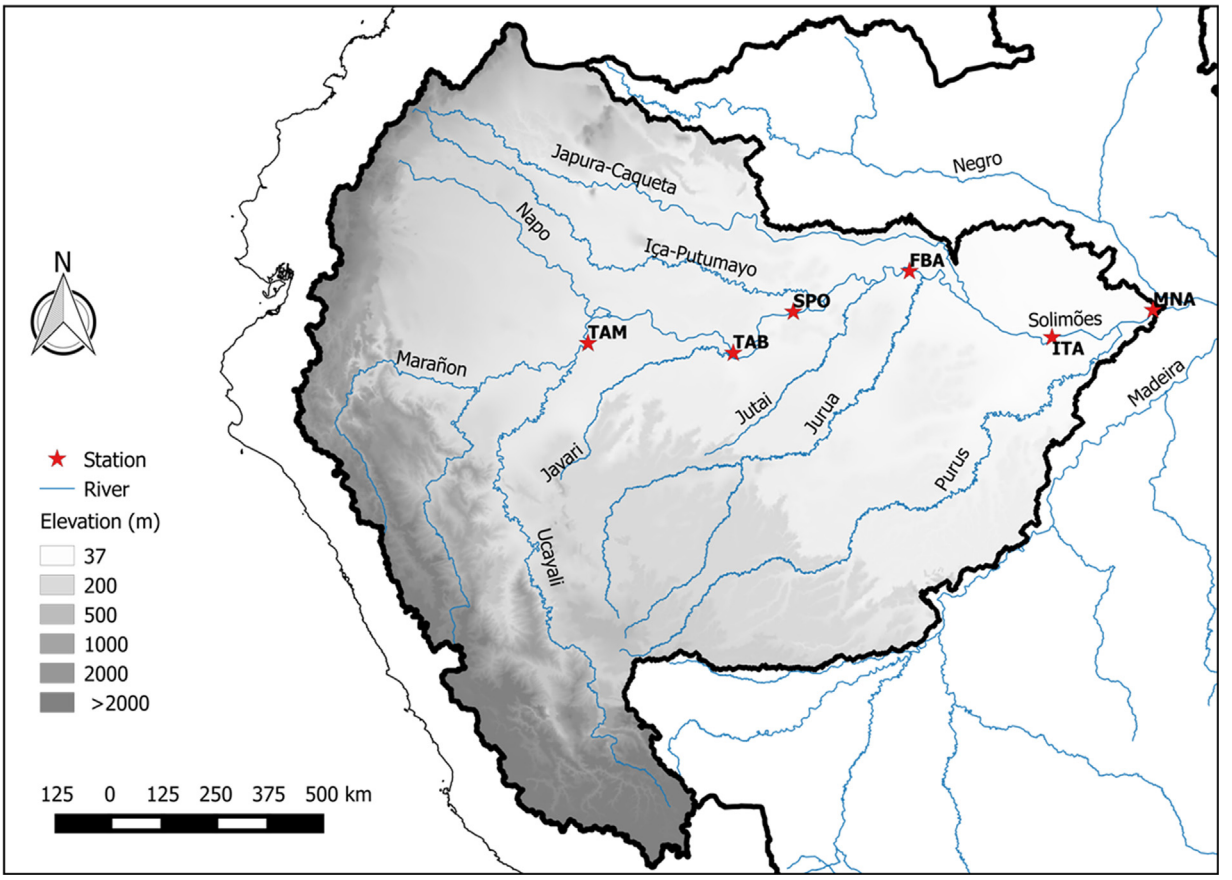

Fig. 1. Location of the Solimões Basin up to Manacapuru (MNA), in the Amazon Basin. The red stars indicate sampling stations.

It has been shown that the optical properties of water are related to water-quality parameters, such as turbidity (Dekker, 1993; Mertes et al., 1993), algal pigments (Gohin et al., 2002; Schalles et al., 1998), and dissolved organic matter (Vodacek et al., 1995). Several studies have successfully demonstrated that remote-sensing techniques may be used for suspended sediment monitoring in water bodies (Doxaran et al., 2002; Martinez et al., 2015; Mertes et al., 1993; Miller and Cruise, 1995; Montanher et al., 2014; Novo et al., 1991; Ritchie et al., 1989) In particular, it has been shown that the Moderate Resolution Imaging Spectroradiometer (MODIS) on board the TERRA and AQUA satellites is well adapted for monitoring suspended sediments in the Amazon basin (Espinoza-Villar et al., 2012, 2013; Kilham and Roberts, 2011; Mangiarotti et al., 2013; Martinez et al., 2009, 2015; Park and Latrubesse, 2014). Each MODIS sensor provides near-daily coverage of the tropics, a major advantage when dealing with regions marked by significant cloud cover such as the Amazon. MODIS data allow the analysis of long time series of suspended sediment concentration (SSS), filling data from field monitoring (Espinoza-Villar et al., 2012; Martinez et al., 2009) and creating a virtual station network (Espinoza-Villar et al., 2013). In this study, MODIS remote-sensing images were used to fill field data and create a virtual station network along the Solimões River. Using more than 13 years of MODIS data, we present results showing, for the first time, the temporal and spatial dynamics of the Solimões River sediment discharge along its entire stretch.

2. Study area

The drainage area covers an area of 2.2×10^6 km^2, and the distance between the TAM and MNA stations is 2050 km (Fig. 1). The northern and southern tributaries between the TAM and MNA gauging stations are characterized by different hydrological regimes. Northern tributaries (Napo, Içá-Putumayo and Japurá Rivers) show a flood peak between May and July and a low-water stage between September and October. Southern tributaries (Javarí, Jutaí, Juruá/Caqueta and Purus Rivers) show a flood peak season between February and April and a low-water period in August–September (Espinoza et al., 2009). This study uses data from six stations located downstream from the confluence with each major tributary river (Fig. 1).

The integration of the contrasted flood regimes from the northern and southern tributaries shows a unimodal flow regime in the Amazonas–Solimões River. At the TAM station, the flood peak occurs in April–May, while at the MNA station the flood peak occurs two months later, in June–July. The low-water period at the TAM station occurs from September to October; at the MNA station, the low-water stage generally occurs one month later, between October and November (Espinoza et al., 2011). Table 1 shows the stations included in this study, which uses field data and remote-sensing data.

3. Data and method

3.1. The SO-HYBAM field campaigns in the Solimões River

From 2007 to 2011, hyperspectral radiometric measurements were performed using spectroradiometers during ten cruises. The purpose of these trips was to collect field data along the Solimões River during different hydrological periods. During these cruises, spectral reflectance data and 76 water samples were collected simultaneously.

The suspended sediment samples were processed using the same protocol used for the processing of the 10-day water samples collected by the SO-HYBAM measurement network (Espinoza-Villar, 2013; Filizola, 2003). Average suspended sediment (ASS) was estimated using nine 500-ml water samples collected at three verticals and three different depths from the surface to the bottom of the water column. The radiometric measurements were performed with TriOS-RAMSES hyperspectral spectroradiometers. The instruments were attached to the prow of the ship, facing forward to minimize ship shadow and reflection. The acquisition geometry recommended by Mobley (1999) from numerical modelling was followed. Field reflectance data were used to simulate the MODIS surface reflectance in the red and near-infrared (NIR) channels.

The river's discharge was measured with a 600-kHz Acoustic Doppler Current Profiler (ADCP) (Callède et al., 2000; Guyot et al., 1998); 97 discharge measurements were made during the 2007–2013 period in the Upper Solimões. National institutions that are partners of SO-HYBAM (the National Meteorology and Hydrology Service–SENAMHI, in Peru and the National Water Agency–ANA and Geological Service in Brazil–CPRM) continuously monitor the TAM and MNA gauging stations.

Table 1
Virtual station network along the Solimões River considered for this study. For each station, latitude (Lat), longitude (Lon), monthly maximum discharge (Q_{max}), monthly minimum discharge (Q_{min}), and annual mean discharge (Q_{mean}) are indicated. The data have been calculated from the SO-HYBAM database available at http://www.ore-hybam.org.

Station	Code	Lat	Lon	Drainage Area $\times 10^3$ km^2	Qmax m^3/s	Qmin m^3/s	Qmean m^3/s
Tamshiyacu	TAM	−4.004	−73.165	726	54,800	10,000	29,600
Tabatinga	TAB	−4.218	−69.962	890	58,500	10,100	37,800
São Paulo de Olivença	SPO	−3.448	−68.897	940	82,500	16,800	47,700
Fonte Boa	FBA	−2.482	−66.049	1159	93,900	16,700	57,000
Itapeua	ITA	−4.053	−63.028	1760	128,200	43,000	84,700
Manacapuru	MNA	−3.312	−60.630	2242	160,000	40,800	103,800

3.2. Satellite data

Surface reflectance MODIS sensors were used in this study. The MODIS data products MOD09Q1 (Terra on-board sensor) and MYD09Q1 (Aqua on-board sensor) provide calibrated reflectance for two radiometric bands measured at a 250-m pixel special resolution while offering near-daily time coverage over tropical areas (http://modis.gsfc.nasa.gov). Bands 1 and 2 are centred at 645 and 858.5 nm, respectively. The MODIS surface reflectance 8-day composite data were acquired from March 2000 to December 2013 from the NASA Warehouse Inventory Search Tool (WIST) data gateway.

In this paper, we use the computational algorithm MOD3R (MODIS River Reflectance Retrieval) developed by IRD–HYBAM (Espinoza-Villar, 2013). This tool automatically retrieves the reflectance of the "pure" pixels of water, facilitating calculation for a large number of images. MOD3R has been used successfully in several studies (Espinoza-Villar et al., 2012, 2013; Martinez et al., 2009) and is freely available at http://www.ore-hybam.org/.

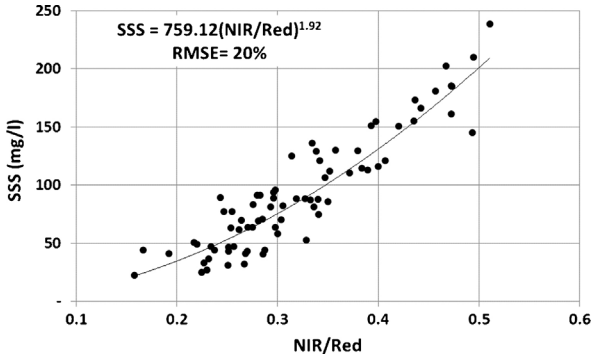

Fig. 2. Scatter plot showing simulated satellite data (NIR/Red) and field data for the 2007–2011 period. The regression equation and relative RMSE are indicated.

3.3. SSS estimation

3.3.1. The SSS-reflectance relationship

The relationship between SSS and reflectance was calculated using field data collected during the sampling cruises. The field spectroradiometric measurements collected along the Solimões River were used to simulate the MODIS radiometric band. The reflectance ratio between the infrared and red bands showed the best retrieval model performance, as shown by previous authors (Doxaran et al., 2002, Espinoza-Villar et al., 2013; Martinez et al., 2015) (Fig. 2). Fig. 2 shows the reflectance ratio-SSS concentration matchups based on the 76 spectroradiometric measurements. Over the concentration range sampled (22–238 mg/l), with a mean value of 92 mg/l, the relative Root Mean Square Error (RMSE) is of 20% or 18.87 mg/l.

SSS time series retrieved from satellite data

SSS concentrations for all stations were retrieved from the MODIS 8-day composite time series using the retrieval model defined in the previous section (Fig. 2). Fig. 3 shows the seasonal SSS concentration cycle related to the annual monomodal flood over the 2000–2013 period. A general decrease in SSS concentration from upstream to downstream is observed. At the TAM station, the SSS concentration peak is greater than 600 mg/l, while at the MNA station, the SSS peak is less than 300 mg/l. This phenomenon is primarily related to dilution by sediment-poor waters from tributaries, but it may also be caused by the settling of sediment in the floodplain (Laraque et al., 2005).

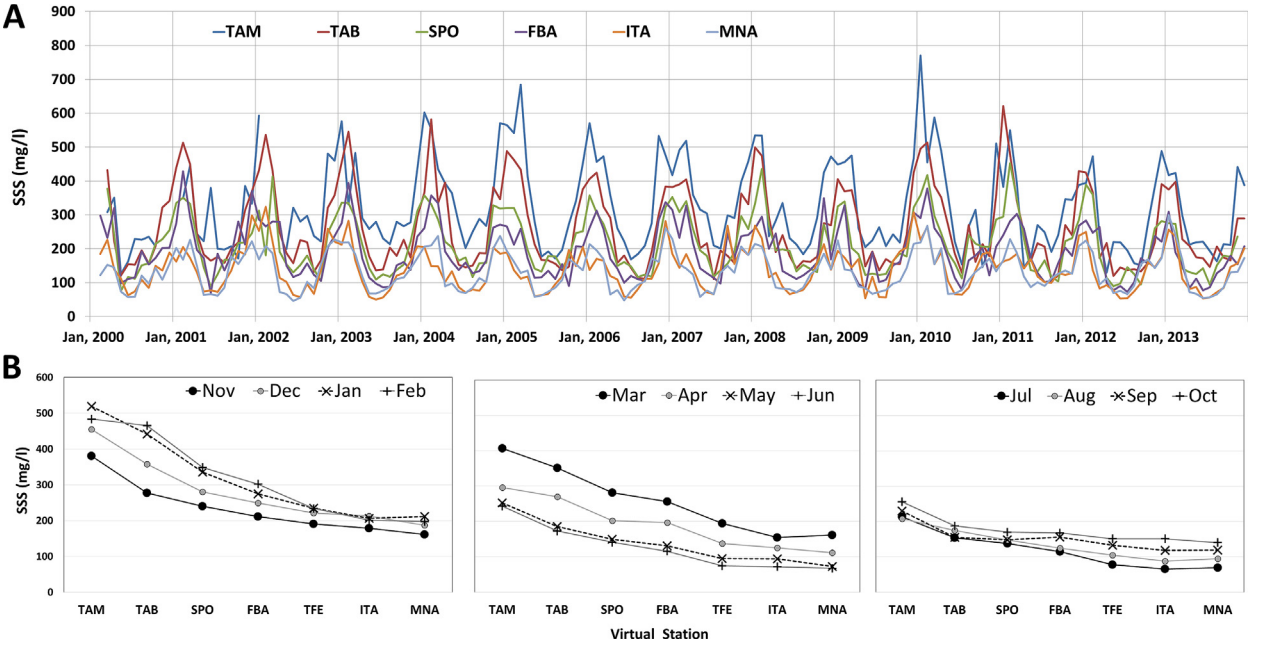

Fig. 3. The satellite-derived SSS concentration assessed along the Solimões River for six gauging stations. A. Monthly SSS concentration time series for the 2000–2013 period. B. Average monthly SSS as a function of distance from upstream and three different hydrological periods.

On average, for the entire time series, the SSS concentration at MNA is by 40% lower than at TAM. This decrease varies seasonally, from 28% in June (flood peak) to 55% in October (low-water stage). This overall SSS decrease pattern along the stream is not observed between the ITA and MNA stations, where there is a slight increase in the SSS concentration twice each year, from January to March and from July to September (Fig. 3b).

3.3.2. Validation

The HYBAM observatory has been providing 10-day SSS concentration estimates for the Solimões River since 1995 at MNA and since 2004 at TAM. The concentration peak usually occurs at both stations between January and February, while the lowest concentrations are recorded between September and October. During the study period, the maximum SSS concentrations were 977 mg/l at the TAM station (January 2010) and 392 mg/l at the MNA station (February 2010).

The satellite-retrieved SSS time series was compared with SO-HYBAM field measurement data at both the TAM and MNA stations. Fig. 4 compares the satellite-derived and network SSS samples at TAM and MNA for the 2000-2013 period. High correlation was found (correlation coefficient $r = 0.89$), which shows that satellite data make it possible to monitor temporal variability regardless of cloud cover, even when the cloud cover is very strong during the rainy period. During the 2000–2013 period, 233 satellite-field SSS matchups were retrieved, with a delay between MODIS and HYBAM data collection of less than 5 days. The 233 matchups had a relative RMSE of 32% (70.23 mg/l) for a SSS concentration data of 50–700 mg/l.

3.4. Sediment discharge estimation

3.4.1. The average concentration of suspended sediments (ASS) at the river reach

ASS was calculated from water samples acquired in the full river section during the SO-HYBAM fieldwork. The samples were taken in various vertical and 3 to 5 depths per vertical in the river section. Fig. 5 shows the relationship between the SSS data and the ASS data for all the river reach sampled along the Solimões River, representing 93 different samplings. A simple linear regression model fits well the SSS/ASS relationship, with a coefficient of determination (r^2) of 0.86. The ASS data were calculated for all stations from satellite-retrieved SSS data (Fig. 4), using the equation shown in Fig. 5. The monthly average ASS concentrations were obtained by averaging the MODIS-derived 8-day estimates over each month.

3.4.2. Sediment discharge (Q_s)

For each station, the monthly average river sediment discharge (Q_s) is calculated by multiplying the monthly discharge records and the monthly average ASS concentration. Fig. 6A shows the monthly average sediment discharge time series through the Solimões River at the TAM, TAB, SPO, FBA, ITA and MNA stations from satellite images. Upstream, Q_s shows little variation from the TAM station to SPO. Downstream, at the ITA and MNA stations, however, a significant increase in Q_s can be observed from January to March and from July to September. The largest value of Q_s registered over the observed period occurred in April 2010 (ITA station) and February 2013 (ITA and MAN stations), exceeding 130 Mt/month in both cases.

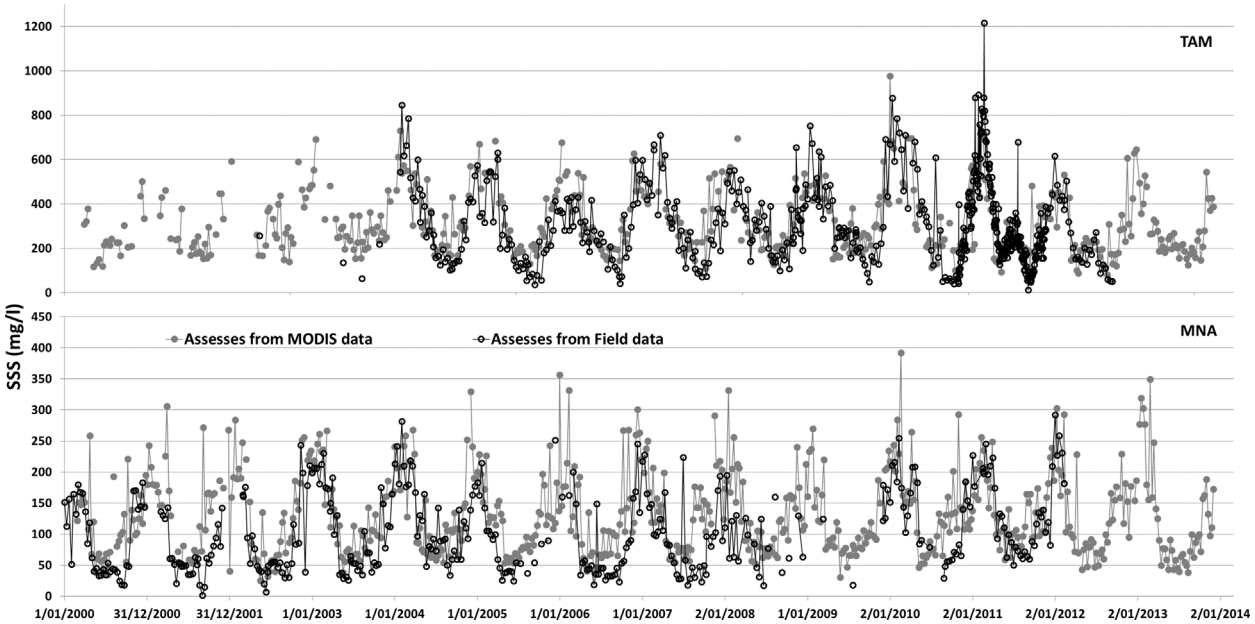

Fig. 4. SSS concentration time series at TAM and MNA stations, retrieved from 8-day composite MODIS images (blue dots) and 10-day HYBAM field samples taken between 2000 and 2013 (red dots).

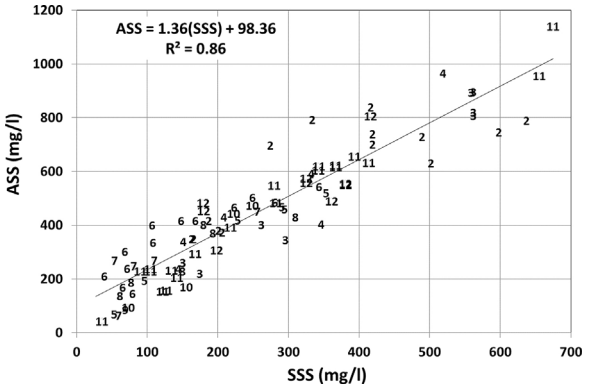

Fig. 5. Relationship between suspended sediment concentration (SSS) and average suspended sediments (ASS) in cross-section for six gauging stations. The linear regression equation and coefficient of determination are indicated. The numbers indicate the months (1 = January to 12 = December).

Fig. 6B shows the average seasonal Q_s variation calculated over the 2000–2013 period. At all stations, peak river sediment discharge is observed between January and March, which confirms that most of the sediment passing through the Solimões River comes from the TAM station or southern rivers with similar hydrological regimes. At the ITA and MNA stations, a bimodal regime is found, with a second smaller peak of river sediment discharge from June to September. Fig. 6B also shows a strong increase in Q_s between the FBA and ITA stations, particularly considering the July–October season; indeed, Q_s at ITA is about by 70% higher than Q_s at FBA, considering average values for the 2000–2013 period.

Fig. 6C compares satellite-derived Q_s with field measurements made at various locations along the Solimões River by the HYBAM monitoring program. Satellite-derived Q_s corresponds to the monthly average expressed in Mt/day, while field measurements correspond to instantaneous data, also expressed in Mt/day. Despite the time difference between the two protocols, a comparison of the two methods showed excellent agreement ($r = 0.93$), with an RMSE of 0.48 Mt/day (27% relative to the sample average). These results confirm that MODIS-derived Q_s estimates correspond closely with independent Q_s field assessments, as documented in previous studies (Espinoza-Villar et al., 2012, 2013; Martinez et al., 2009).

4. Discussion

MODIS satellite images were used to generate SSS concentration and Q_s time series for six virtual stations during the 2000–2013 period. The comparison between satellite and field data shows excellent agreement for both SSS concentration and Q_s. Table 2 shows the satellite-derived sediment discharge and the mean SSS concentration at every virtual station studied along the Solimões River. The annual river sediment discharge upstream at the TAM station is 521 Mt/year, which corresponds to 58% of

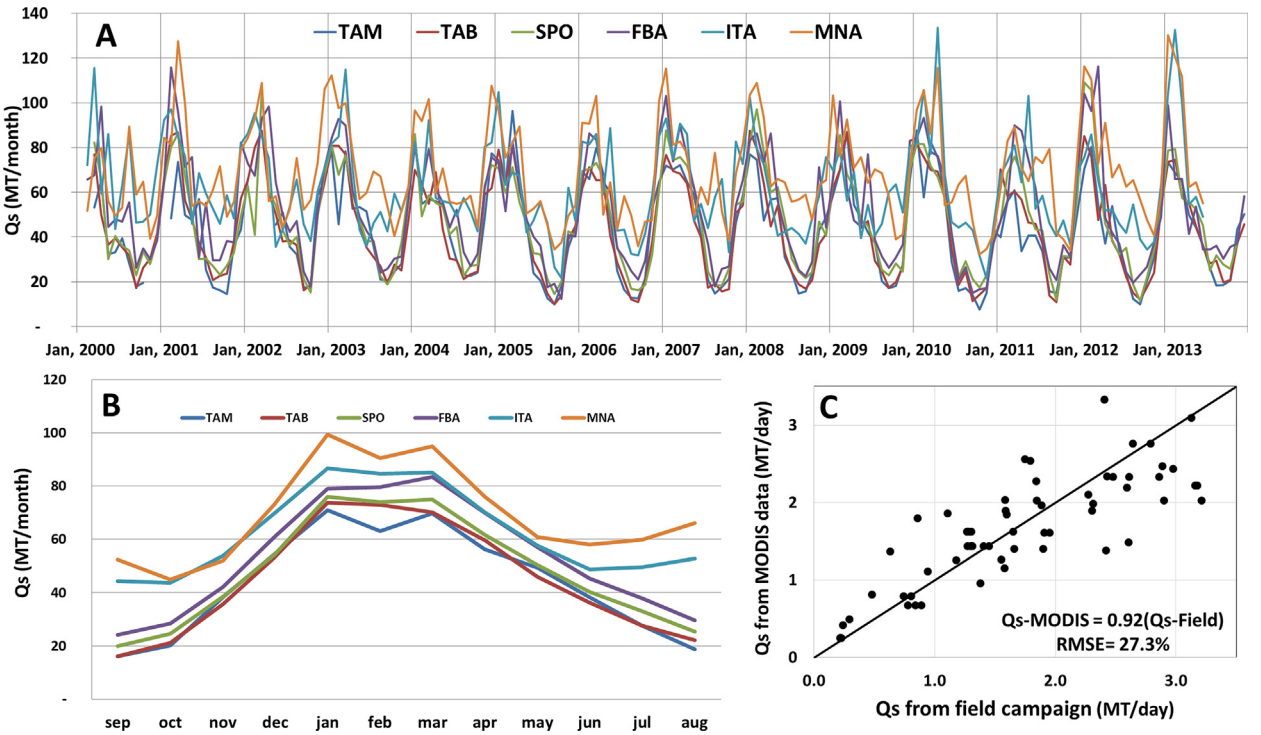

Fig. 6. Monthly average discharge at each station, from Tamshiyacu (TAM) to Manacapuru (MNA), through the Solimões River. A. Yield discharge time series (Q_s) for each station during the 2000–2013 period. B. Mean monthly values during the annual cycle (September to August). C. Relationship between Q_s assessed from field-sampling campaigns and Q_s assessed from MODIS data. The equations from linear regression and the RMSE value are indicated.

Table 2
Characteristics of the hydrological gauging stations used in this study, showing the mean annual SSS (mg/l), Q_s (Mt/year) and specific yield discharge (t/year·km^2).

Station	SSS mg/l	Q_s Mt/Year	Specific yield discharge t/(year·km^2)	Correlation of Qs with MNA r^2
Tamshiyacu (TAM)	329	521	718	0.03
Tabatinga (TAB)	266	541	603	0.26[a]
São Paulo de Olivença (SPO)	215	574	566	0.65[b]
Fonte Boa (FBA)	192	643	501	0.62[b]
Itapeua (ITA)	139	742	418	0.50[b]
Manacapuru (MNA)	133	825	368	–

The coefficients of correlation between the annual Q_s of each station with MNA are indicated.
[a] $P \leq 0.1$.
[b] $P \leq 0.01$

the river sediment discharge downstream at MNA. Between the same stations, the river water discharge increases by 350% on average for the study period. These estimates are consistent with previous results from Armijos et al. (2013), who calculated annual river sediment discharge values of 520 and 541 Mt/year at the TAM and TAB stations, respectively, during the 2004–2010 period.

The variations in river sediment discharge recorded along the stream may be due to dilution, sedimentation and resuspension processes (Meade et al., 1985). Dilution is caused by tributaries, which bring low sediment discharge, but which significantly increase discharge in the main stream at their outlets. Sedimentation may occur either through sediment deposition on the floodplain during overbanking or in the main channel itself. Resuspension may originate from remobilization of material in the large floodplain system, an area estimated to exceed 100 000 km^2 along the Solimões River. These processes may occur in succession or simultaneously, depending on the river stretch, which explains why the interannual Qs at TAM does not correlate with Q_s at MNA ($r = 0.17$; Table 2).

River sediment discharge shows little variation along the mainstream from the TAM station to the SPO station. We assess an annual river sediment discharge at SPO station of 574 Mt/year. Our estimates is close to the calculation proposed by Dunne et al. (1998) based on field-sampling campaigns from 1981 to 1984 that assessed a sediment discharge of 616 Mt/year for the same station. The apparent stability of the sediment discharge along the TAM–SPO stretch may hide complex interactions between sedimentation processes and lateral sediment inputs from the Napo and Javari Rivers, which are impossible to discriminate with our data. The annual river sediment discharge between the SPO and FBA stations shows an average 12% increase, which is probably related to the Içа/Putumayo River northern tributary inputs, especially during the second part of the hydrological cycle from March to August. The satellite-derived estimates match well the field estimates provided by Dunne et al. (1998), who found a 10% increase on the same river stretch from SPO to near the FBA station. Between the FBA and ITA stations, the Solimões River receives significant inputs from two major tributaries: the Japura/Caqueta River and the Juruá River. The Japura/Caqueta River, a northern tributary, shows peak water discharge in July, while the Jurua River, a southern tributary, shows peak water discharge in April (Espinoza et al., 2009). The 15% sediment discharge along this stretch is probably mostly induced by sediment inputs from those two tributaries. It is worth noting, however, that there is no sediment discharge increase from the FBA to ITA stations between March and June, which probably denotes significant sedimentation processes in the local floodplain during that period. Instead, there is a large sediment discharge increase on the same stretch during the last part of the hydrological cycle (84%), from August to November, which may reveal important resuspension processes during the low-water period of recently deposited sediment in the floodplain. Satellite-derived estimates match again very well previous estimates from Dunne et al. (1998) that assessed a sediment discharge of 731 Mt/year at ITA station.

Downstream, the river sediment discharge at the ITA and MAN stations shows a temporal pattern that is very different from upstream, with two separate peaks. From January to March, a significant sediment discharge increase is seen, probably induced by the sediment inputs from the Purus River, a southern tributary that shows a peak discharge during that period.

Our results provide a mean sediment discharge at MNA of around 825 Mt/year, which suggests a higher sediment budget comparing with some previous studies. However, our results are in accordance with previous estimations of sediment discharge at TAM (520 Mt/year), which is very close to those calculated by Armijos et al. (2013) in this station (550 Mt/year). According to these results, our estimation of sediment discharge at MNA appears coherent considering the contribution of several tributaries between TAM and MNA (Napo, Javarí, Jutaí, Juruá, Japurá, Içá-Putumayo and Purus). The higher sediment budget estimated in our study compared with previous works can be attributed to the better monitoring of the hydrological year provided in this study. Indeed, our results document for the first time a second peak of sediment discharge at ITA and MNA during August–September. These new findings confirm the usefulness of remote sensing for the improvement of our understanding of hydrological dynamics. The second peak can be attributed to the resuspension of sediments deposited during the low-water

period (when sediment charge is higher than the hydraulic capacity of the river). These sediments can be washloaded during July-September, when the northern rivers provide high water discharges with low sediment concentrations. In addition, the second peak can also be associated with sediment supply from the floodplains (Ritchie et al., 1989) or from the lateral bank erosion, as suggested by Dunne et al. (1998) and Alsdorf et al. (2010). However, the role of the floodplains over sediment discharge is yet poorly known.

Interestingly, previous results produced by Dunne et al. (1998) matched well the satellite-derived sediment discharge estimates for all stations from SPO to ITA and the upstream-downstream evolution, except for the MAN station, where a significant discrepancy is found. Those authors assessed a sediment river discharge of 697 Mt/year at MAN station, while we assess a sediment discharge of 825 Mt/year. However, Dunne et al. (1998) basically assessed river sediment discharge by regressing SSS concentration against discharge. As the secondary sediment discharge peak at MAN station appears during the declining water period (from July to October), Dunne's calculation will significantly underestimate the sediment discharge during that period. On the contrary, as our sediment discharge calculation is based on the measured SSS concentration, our sediment discharge assessment is not affected by the SSS/discharge relationship. These different modes of calculation likely explain why Dunne et al. (1998) did not catch this sediment increase from ITA to MAN, as we have observed it in this work.

The satellite data revealed the complex sediment transport processes occurring along the stream of the Solimões River, particularly a significant sediment discharge increase in the downstream part of the Solimões River. We retrieved the highest peak sediment concentrations (Fig. 3A) in 2005 and 2010, when historic droughts were recorded in the Amazon River basin (Marengo and Espinoza, 2015), with dramatic high impacts over the Peruvian Amazon (Espinoza et al., 2011). These SSS concentration peaks during these dry years are probably due to lower dilution by tributaries, which brought smaller amounts of water to the mainstream. These observations show that sediment discharge monitoring will be important to assess the evolution of the world largest catchment following the impact of global and regional changes.

Acknowledgements

The authors would especially like to acknowledge all their colleagues of the national hydrological services, the National Water Agency (ANA) and the Geological Survey of Brazil (CPRM) in Brazil and the National Weather and Hydrology Service of Peru (SENAMHI), who are partners in the SO-HYBAM program (the Observation Service for the Geodynamical, Hydrological and Biogeochemical Control of Erosion/Alteration and Material Transport in the Amazon Basin), and who contributed to collection and analysis of the data used in this study.

References

Alsdorf, D., Han, S.-C., Bates, P., Melack, J., 2010. Seasonal water storage on the Amazon floodplain measured from satellites. Remote Sens. Environ. 114, 2448–2456, http://dx.doi.org/10.1016/j.rse.2010.05.020.

Armijos, E., Crave, A., Vauchel, P., Fraizy, P., Santini, W., Moquet, J.S., Guyot, J.-L., 2013. Suspended sediment dynamics in the Amazon River of Peru. J South Am. Earth Sci. 44, 75–84.

Callède, J., Kosuth, P., Guyot, J.-L., Guimarães, V.S., 2000. Discharge determination by acoustic doppler current profilers (ADCP): a moving bottom error correction method and its application on the river Amazon at Obidos. Hydrol. Sci. J. 45 (6), 911–924.

Dekker, A.G., 1993. Detection of optical water quality parameters for eutrophic waters by high resolution Remote sensing. PhD thesis, Proefschrift Vrije Universiteit (Free University), Earth and Life Sciences, Amsterdam, The Netherlands.

Doxaran, D., Froidefond, J.M., Castaing, P., 2002. A reflectance band ratio used to estimate suspended matter concentrations in sediment-dominated coastal waters. Int. J. Remote Sens. 23 (23), 5079–5085.

Dunne, T., Mertes, L.A., Meade, R.H., Richey, J.E., Forsberg, B.R., 1998. Exchanges of sediment between the flood plain and channel of the Amazon River in Brazil. Geol. Soc. Am. Bull. 110 (4), 450–467.

Espinoza-Villar, R., 2013. Suivi de la dynamique spatiale et temporelle des flux sédimentaires dans le bassin de l'Amazone à partir d'images satellite. PhD thesis, Université Toulouse 3-Paul-Sabatier, Toulouse, France.

Espinoza, J.C., Guyot, J.-L., Ronchail, J., Cochonneau, G., Filizola, N., Fraizy, P., Vauchel, P., 2009. Contrasting regional discharge evolutions in the Amazon basin (1974-2004). J. Hydrol. 375 (3), 297–311.

Espinoza, J.C., Ronchail, J., Guyot, J.-L., Junquas, C., Vauchel, P., Lavado, W., Pombosa, R., 2011. Climate variability and extreme drought in the upper Solimões River (western Amazon Basin): Understanding the exceptional 2010 drought. Geophys. Res. Lett. 38 (13) .

Espinoza, J.C., Ronchail, J., Guyot, J.-L., Junquas, C., Drapeau, G., Martinez, J.-M., Espinoza-Villar, R., 2012. From drought to flooding: understanding the abrupt 2010-11 hydrological annual cycle in the Amazonas River and tributaries. Environmental Res. Lett. 7 (2), 024008.

Espinoza-Villar, R.E., Martinez, J.-M., Guyot, J.-L., Fraizy, P., Armijos, E., Crave, A., Lavado, W., 2012. The integration of field measurements and satellite observations to determine river solid loads in poorly monitored basins. J. Hydrol. 444, 221–228.

Espinoza-Villar, R.E., Martinez, J.-M., Le Texier, M., Guyot, J.-L., Fraizy, P., Meneses, P.R., de Oliveira, E., 2013. A study of sediment transport in the Madeira River, Brazil, using MODIS remote-sensing images. J South Am. Earth Sci. 44, 45–54.

Filizola, N.P., 1999. O fluxo de sedimentos em suspensão nos rios da bacia Amazônica Brasileira. ANEEL.

Filizola, N., 2003. Transfert sédimentaire actuel par les fleuves amazoniens. Université Toulouse 3- Paul-Sabatier, Toulouse, France, 292 p.

Filizola, N., Guyot, J.-L., 2009. Suspended sediment yields in the Amazon basin: an assessment using the Brazilian national data set. Hydrol. Processes 23 (22), 3207–3215.

Filizola, N., de Oliveira, E., Wittmann, H., Guyot, J.-L., Martinez, J.-M., 2011. The significance of suspended sediment transport determination on the Amazonian hydrological scenario. INTECH Open Access Publisher.

Gibbs, R.J., 1967. Amazon River: Environmental factors that control its dissolved and suspended load. Science 156 (3783), 1734–1737.

Gohin, F., Druon, J.N., Lampert, L., 2002. A five channel chlorophyll concentration algorithm applied to SeaWiFS data processed by SeaDAS in coastal waters. Int. J. Remote Sens. 23 (8), 1639–1661.

Guyot, J.-L., Filizola, N., Guimaraes, V., 1998. Amazon suspended sediment yield measurements using an Acoustic Doppler Current Profiler (ADCP): first results. IAHS Publ, 109–116.

Guyot, J.-L., Filizola, N., Laraque, A., 2005. Régime et bilan du flux sédimentaire de l'Amazone à Óbidos (Pará, Brésil) de 1995 à 2003. Sediments Budgets 1. IAHS Publ. 291, 347.

Guyot, J.-L., Bazan, H., Fraizy, P., Ordonez, J.J., Armijos, E., Laraque, A., 2007. Suspended sediment yields in the Amazon basin of Peru: a first estimation, 314, IAHS Publ, pp. 3.

Kilham, N.E., Roberts, D., 2011. Amazon River time series of surface sediment concentration from MODIS. Int J Remote Sens. 32 (10), 2659–2679.

Laraque, A., Filizola, N., Guyot, J.-L., 2005. Variations spatio-temporelles du bilan sédimentaire dans le bassin Amazonien Brésilien, à partir d'un échantillonnage décadaire. IAHS-AISH Publ, 250–258.

Mangiarotti, S., Martinez, J.-M., Bonnet, M.P., Buarque, D.C., Filizola, N., Mazzega, P., 2013. Discharge and suspended sediment flux estimated along the mainstream of the Amazon and the Madeira Rivers (from in

situ and MODIS Satellite Data). Int. J. Appl. Earth Obs. Geoinform. 21, 341–355.
Marengo, J.A., Espinoza, J.C., 2015. Extreme seasonal droughts and floods in Amazonia: causes, trends and impacts. Int. J. Climatol. 36, 1033–1050.
Martinez, J.-M., Guyot, J.-L., Filizola, N., Sondag, F., 2009. Increase in suspended sediment discharge of the Amazon River assessed by monitoring network and satellite data. Catena 79 (3), 257–264.
Martinez, J.-M., Espinoza-Villar, R., Armijos, E., Silva Moreira, L., 2015. The optical properties of river and floodplain waters in the Amazon River Basin: Implications for satellite-based measurements of suspended particulate matter. J Geophys Res. Earth Surf. 120 (7), 1274–1287.
Meade, R.H., Nordin, C.F., Curtis, W.F., Rodrigues, F.M.C., Do Vale, C.M., Edmond, J.M., 1979. Sediment loads in the Amazon River. Nature 278, 161–163.
Meade, R.H., Dunne, T., Richey, J.E., Santos, U.D.M., Salati, E., 1985. Storage and remobilization of suspended sediment in the lower Amazon River of Brazil. Science 228 (4698), 488–490.
Mertes, L.A., Smith, M.O., Adams, J.B., 1993. Estimating suspended sediment concentrations in surface waters of the Amazon River wetlands from Landsat images. Remote Sens. Environ. 43 (3), 281–301.
Mertes, L.A., Dunne, T., Martinelli, L.A., 1996. Channel-floodplain geomorphology along the Solimões-Amazon River. Brazil. Geol. Soc. Am. Bull. 108 (9), 1089–1107.
Miller, R.L., Cruise, J.F., 1995. Effects of suspended sediments on coral growth: evidence from remote sensing and hydrologic modeling. Remote Sens. Environ. 53 (3), 177–187.
Mobley, C.D., 1999. Estimation of the remote-sensing reflectance from above-surface measurements. Appl. Opt. 38 (36), 7442–7455.
Molinier, M., Guyot, J.-L., De Oliveira, E., Guimarães, V., 1996. Les régimes hydroiogiques de l'Amazone et de ses affluents. IAHS Publ, 209–222.
Montanher, O.C., Novo, E.M., Barbosa, C.C., Rennó, C.D., Silva, T.S., 2014. Empirical models for estimating the suspended sediment concentration in Amazonian white water rivers using Landsat 5/TM. Int. J. Appl. Earth Observ. Geoinform. 29, 67–77.
Novo, E.M.L.M., Steffen, C.A., Braga, C.Z.F., 1991. Results of a laboratory experiment relating spectral reflectance to total suspended solids. Remote Sens. Environ. 36 (1), 67–72.
Park, E., Latrubesse, E.M., 2014. Modeling suspended sediment distribution patterns of the Amazon River using MODIS data. Remote Sens. Environ. 147, 232–242.
Richey, J.E., Meade, R.H., Salati, E.D.A.H., Devol, A.H., Nordin, C.F., Dos Santos, U., 1986. Water discharge and suspended sediment concentrations in the Amazon River: 1982-1984. Water Resour. Res. 22 (5), 756–764.
Ritchie, J.C., Schiebe, F.R., Cooper, C.M., 1989. Landsat digital data for estimating suspended sediment in inland water. Int. Ass. Hydrol. Sci. 182, 151–158.
Ronchail, J., Guyot, J., Villar, J.C.E., Fraizy, P., Cochonneau, G., De Oliveira, E., Ordenez, J.J., 2006. Impact of the Amazon tributaries in major floods at Obidos, 303, IAHS Publ, pp. 220.
Schalles, J.F., Gitelson, A.A., Yacobi, Y.Z., Kroenke, A.E., 1998. Estimation of chlorophyll a from time series measurements of high spectral resolution reflectance in an eutrophic lake. J. Phycol. 34 (2), 383–390.
Vodacek, A., Hogel, F.E., Swift, R.N., Yungel, J.K., Peltzer, E.T., Blough, N.V., 1995. The use of in situ and airborne fluorescence measurements to determine UV absorption coefficients and DOC concentrations in surface waters. Limnol. Oceanogr. 40 (2), 411–415.